Cerebral Cortex April 2012;22:926–936
doi:10.1093/cercor/bhr164
Advance Access publication July 1, 2011

Estradiol Rapidly Rescues Synaptic Transmission from Corticosterone-induced Suppression via Synaptic/Extranuclear Steroid Receptors in the Hippocampus

Yuuki Ooishi[1], Hideo Mukai[1,2], Yasushi Hojo[1,2,3], Gen Murakami[1,3], Yoshitaka Hasegawa[1], Tomu Shindo[1], John H. Morrison[4], Tetsuya Kimoto[1] and Suguru Kawato[1,2,3,5]

[1]Department of Biophysics and Life Sciences, Graduate School of Arts and Sciences and [2]Core Research for Evolutional Science and Technology Project of Japan Science and Technology Agency and [3]Bioinformatics Project of Japan Science and Technology Agency, The University of Tokyo, Tokyo 153-8902, Japan, [4]Kastor Neurobiology of Aging Laboratories, Fishberg Research Center for Neurobiology, Mount Sinai School of Medicine, New York, NY 10029, USA and [5]National MEXT Project in Special Coordinate Funds for Promoting Science and Technology, The University of Tokyo, Tokyo 153-8902, Japan

Address correspondence to Dr Suguru Kawato, Department of Biophysics and Life Sciences, Graduate School of Arts and Sciences, The University of Tokyo, 3-8-1 Komaba, Meguro, Tokyo 153-8902, Japan. E-mail: kawato@phys.c.u-tokyo.ac.jp

We investigated rapid protection effect by estradiol on corticosterone (CORT)-induced suppression of synaptic transmission. Rapid suppression by 1 μM CORT of long-term potentiation (LTP) at CA3–CA1 synapses was abolished via coperfusion of 1 nM estradiol. N-methyl-D-aspartate (NMDA) receptor-derived field excitatory postsynaptic potential (NMDA-R-fEPSP) was used to analyze the mechanisms of these events. Estradiol abolished CORT-induced suppression of NMDA-R-fEPSP slope. This CORT-induced suppression was abolished by calcineurin inhibitor, and the rescue effect by estradiol on the CORT-induced suppression was inhibited by mitogen-activated protein (MAP) kinase inhibitor. The CORT-induced suppressions of LTP and NMDA-R-fEPSP slope were abolished by glucocorticoid receptor (GR) antagonist, and the restorative effects by estradiol on these processes were mimicked by estrogen receptor α (ERα) and ERβ agonists. Taken together, estradiol rapidly rescued LTP and NMDA-R-fEPSP slope from CORT-induced suppressions. A GR→calcineurin pathway is involved in these suppressive effects. The rescue effects by estradiol are driven via ERα or ERβ→MAP kinase pathway. Synaptic/extranuclear GR, ERα, and ERβ probably participate in these rapid events. Mass-spectrometric analysis determined that acute hippocampal slices used for electrophysiological measurements contained 0.48 nM estradiol less than exogenously applied 1 nM. In vivo physiological level of 8 nM estradiol could protect the intact hippocampus against acute stress-induced neural suppression.

Keywords: corticosterone, estradiol, hippocampus, LTP, NDMA receptors

Introduction

Corticosterone (CORT) is secreted from the adrenal cortex in a circadian rhythm and CORT level is elevated upon stress. The hippocampus is a target of CORT modulation, due to high-level expression of glucocorticoid receptor (GR). To date, many studies have investigated the genomic effects of CORT in the hippocampus in order to analyze the chronic stress effects by CORT from the viewpoint of cell damage (Woolley et al. 1990; Watanabe et al. 1992; Reagan and McEwen 1997) or the suppression of synaptic plasticity (Pavlides et al. 2002; Gerges et al. 2004; Hirata et al. 2008). These slow effects are known to be mediated by nuclear GR. On the other hand, CORT also shows acute modulation of hippocampal neuronal activity within 1–2 h. A stress level of CORT application acutely suppresses the population spikes of hippocampal CA1 pyramidal cells (Vidal et al. 1986) and the long-term potentiation (LTP) at hippocampal CA3–CA1 synapses (Alfarez et al. 2002; Shibuya et al. 2003). As an another type of acute stressor, application of corticotropin-releasing hormone, a stress-related hormone, acutely decreases the dendritic spines of hippocampal CA3 neurons within 30 min (Chen et al. 2008).

Contrary to these attenuation effects by CORT on neural activity, a sex hormone 17β-estradol has several protective effects on the brain. Estradiol induces nerve growth (Murphy and Segal 1996) and neuroprotection (Behl et al. 1995; Zhang et al. 2001) via genomic mechanisms mediated by nuclear estrogen receptor (ER). Estradiol also has rapid effects. One hundred nanomolar estradiol enhances the kainate receptor-mediated current of hippocampal CA1 pyramidal cells within 5 min (Gu and Moss 1996). One to 10 nM estradiol increases dendritic spines of CA1 pyramidal cells and enhances long-term depression at hippocampal CA3–CA1 synapses within 2 h (Mukai et al. 2007). Because adult male rat hippocampal neurons synthesize estradiol (Kawato et al. 2002; Hojo et al. 2004), hippocampal synapses may be regulated by hippocampus-derived estradiol in an autocrine manner.

In the current study, we focus on the problem whether estradiol could rapidly rescue synaptic transmission from the acute suppression induced by CORT. Although, as a slow genomic effect, neural damage induced by GR agonist is attenuated by estradiol (Haynes et al. 2003), little is known regarding the mechanisms of the rapid cross talk between estradiol and CORT pathways. Possible involvement of synaptic or extranuclear GR and ER in these effects is investigated via immunoelectron microscopic analysis and western blot. We further analyze the participation of kinase or phosphatase in CORT-induced rapid suppression of synaptic transmission and in the rescue processes by estradiol from the suppression by measuring LTP as well as N-methyl-D-aspartate receptor (NMDAR)-derived currents. Because the steroid concentrations are key factors for these events, they are determined by mass-spectrometric analysis in slices used for electrophysiological measurements.

Materials and Methods

Animals

Twelve-week-old male Wistar rats were purchased from Saitama Experimental Animal Supply (Japan). The experimental procedure of this research was approved by the Committee for Animal Research of University of Tokyo.

Chemicals

Estradiol, CORT, propyr pyrazole triol (PPT), diarylpropionitrile (DPN), dexamethasone (DEX), RU486, U0126, and cyclosporin A (CsA) were purchased from Wako Pure Chemicals (Japan). D-2-Amino-5-phosphonovaleric acid, Ro 25-6981 and 6-cyano-7-nitroquinoxaline-2,3-dione (CNQX) were purchased from Sigma.

Slice Preparation

Rats were deeply anesthetized with ethyl ether and decapitated between 9:00 AM and 10:00 AM when plasma CORT levels are low. Immediately after decapitation, the brain was removed from the skull and placed in ice-cold oxygenated (95% O_2, 5% CO_2) artificial cerebrospinal fluid (ACSF) containing (in millimolar): 124 NaCl, 5 KCl, 1.25 NaH_2PO_4, 2 $MgSO_4$, 2 $CaCl_2$, 22 $NaHCO_3$, and 10 D-glucose; pH was set at 7.4. The hippocampus was dissected and 400-μm thick transverse dorsal slices to the long axis, from the middle third of the hippocampus, were prepared with a vibratome (Dosaka, Japan). These freshly prepared slices were then recovered in ACSF for at least 2 h in order to prepare conventional "acute slices." In electrophysiological experiments, these acute slices were transferred to a recording chamber, submerged, and continuously perfused (2 mL/min) with oxygenated ACSF at 30 °C.

Electrophysiology

Bipolar tungsten stimulating electrodes were placed in the Schaffer collateral/commissural fibers. Upon stimulation (pulse duration: 100 μs), the field excitatory postsynaptic potential (fEPSP) was recorded using a glass microelectrode (1–2 MΩ filled with ACSF) placed in the stratum radiatum of the CA1 area. The input–output curve for fEPSP was determined by gradually increasing the stimulus intensity. The stimulation interval was 20 s. When the responses became saturated, the stimulus intensity that yielded the half maximum fEPSP value was calculated. The maximum slope of the fEPSP was also monitored. For induction of LTP, tetanic stimulation was applied at $t = 0$ min to the Schaffer collaterals (100 Hz for 1 s). After LTP induction, the fEPSP was recorded for 60 min. For investigations of steroid effects, steroids were perfused from $t = -30$ min. NMDA receptor-derived field excitatory postsynaptic potential (NMDA-R-fEPSP) was selectively measured by perfusing 10 μM CNQX (2-amino-3-(5-methyl-3-oxo-1,2- oxazol-4-yl)propanoic acid receptor [AMPAR] inhibitor) contained ACSF with a reduced Mg^{2+} concentration of 0.1 mM. The fEPSP slope was calculated as the slope between 20% and 80% of the fEPSP amplitude. All experimental analog data were amplified using a DAM80 (World Precision Instruments) and converted to digital signals by a DIGIDATA 1322A (Axon Instruments). The data were analyzed with a pCLAMP 9.0 (Axon Instruments). For the induction of paired pulse facilitation (PPF), paired pulse stimulation was applied to the Schaffer collaterals. The stimulation interval was 50 ms.

Postembedding Immunogold Method for Electron Microscopy

Immunoelectroscopic analysis was performed essentially as described elsewhere (Mukai et al. 2007). Rat hippocampus was frozen and sliced coronally. Freeze substitution and low-temperature embedding of the specimens was performed as described previously (Adams et al. 2002). The samples were immersed in uranyl acetate in anhydrous methanol (–90 °C). The samples were infiltrated with Lowicryl HM20 resin (Electron Microscopy Sciences) and polymerization was performed with ultraviolet light. Ultrathin sections were cut using a Reichert–Jung ultramicrotome. For immunolabeling, sections were incubated with primary antibody for GR (a gift from Prof. M. Kawata) (diluted to 1/3000) overnight and incubated with secondary gold-tagged (10 nm) Fab fragment in Tris-buffered saline. Sections were counterstained with 1% uranyl acetate and viewed on a JEOL 1200EX electron microscope (Japan). Images were captured using a charge coupled device camera (Advanced Microscopy Techniques).

Western Immunoblot Analysis

Detailed procedures are described elsewhere (Mukai et al. 2007) and in Supplementary Materials. The blots of purified fractions from hippocampal slices were probed with GR antibody diluted to 1/3000, for 12–18 h at 4 °C, and incubated with horseradish peroxidase (HRP)-conjugated goat antirabbit immunoglobulin G (IgG) (Cell Signaling). The protein bands were detected via enhanced chemiluminescence (ECL) plus western blotting detection reagents (Amersham Biosciences). To obtain high quality images of the chemiluminescence from protein bands using ECL plus, we used a LAS3000 Image Analyzer (Fuji Film, Japan) with a 16-bit wide dynamic range.

Mass-spectrometric Assay of Steroids

To examine how much estradiol and CORT remain in hippocampal slices after 2-h recovery in steroid-free ACSF, we performed mass-spectrometric analysis of estradiol and CORT for acute slices and "the isolated whole hippocampus." Detailed procedures are described elsewhere (Hojo et al. 2009) and in Supplementary Materials. Slices were homogenized and steroid extraction was performed. This extraction was performed by a hexane: ethyl acetate = 2:3 mixture. The steroid extracts were applied to a C_{18} Amprep solid-phase column (Amersham Biosciences). The estradiol or CORT fraction was purified from the eluted steroids using a normal-phase high performance liquid chromatography system (Jasco, Japan) with a silica gel column. To increase the ionization efficiency, estradiol was derivatized into estradiol-3-pentafluorobenzoxy-17-picolinoyl-ester (estradiol-PFBz-picolinoyl) (Hojo et al. 2009). The liquid chromatography-tandem mass spectrometry (LC-MS/MS) system, which consisted of a reverse phase LC coupled with an API 5000 triple-stage quadrupole mass spectrometer (Applied Biosystems), was operated with electron spray ionization in the positive ion mode. The LC chromatographic separation for estradiol-PFBz-picolinoyl and CORT was performed on a Cadenza CD-C_{18} column (Imtakt, Japan). The MS/MS process monitored the m/z transition, from 558 to 339 for estradiol-PFBz-picolinoyl and from 347 to 121 for CORT. $^{13}C_4$-estradiol-PFBz-picolinoyl and d_8-CORT were used as internal standards in order to measure the recovery of steroids and to calibrate the retention time.

Statistical Analysis

All the data used for statistical analysis were expressed as a percentage of the mean fEPSP slope during recording of the baseline (during the 10 min prior to changing the perfusion solution to steroid-including ACSF). Before LTP induction, and in the experiment for NMDA-R-fEPSP, the effects of steroids on fEPSP were analyzed by repeated measures analysis of variance (ANOVA), followed by a paired t-test. The paired t-test was corrected by Bonferroni's method. For LTP analysis, we defined the LTP ratio as the average during the 10 min from $t = 50$ to $t = 60$ min. A one-way ANOVA followed by a Tukey and Kramer's post hoc test were used for multiple comparisons between experimental treatments in LTP experiments. Significance was defined as $^{*}P < 0.05$, $^{**}P < 0.01$.

Results

Rapid Suppressive Effect by CORT on LTP

Slices were perfused for 30 min with CORT prior to LTP induction. The dose dependence of the effect of CORT was investigated using 100 nM, 250 nM, and 1 μM CORT. The magnitude of LTP was 134 ± 3% in control slices ($n = 10$ slices), 131 ± 2% in 100 nM CORT-treated slices ($n = 6$), 128 ± 2% in 250 nM CORT-treated slices ($n = 6$), and 121 ± 3% in 1 μM CORT-treated slices ($n = 14$), respectively (Fig. 1 and Supplementary Fig. S1). CORT significantly reduced LTP at a concentration of 1 μM (Fig. 1*B* and Supplementary Fig. S1). One hundred nanomolar DEX, an agonist of GR, significantly reduced LTP to 122 ± 2% ($n = 5$), while 1 μM CORT in the presence of 10 μM RU486, a GR antagonist, did not decrease LTP (132 ± 3%; $n = 6$) (Fig. 1*B*). It should be noted that RU486 alone did not affect LTP. These results indicated that CORT rapidly suppressed LTP via GR.

To investigate whether CORT affected presynaptic activation, PPF was analyzed. Paired pulses with an interval of 50 ms were applied to induce PPF, and the ratio of the fEPSP slope evoked by the second stimulus to that of the first was calculated. No significant change was observed in PPF ratio, between before CORT perfusion, after CORT perfusion, and after

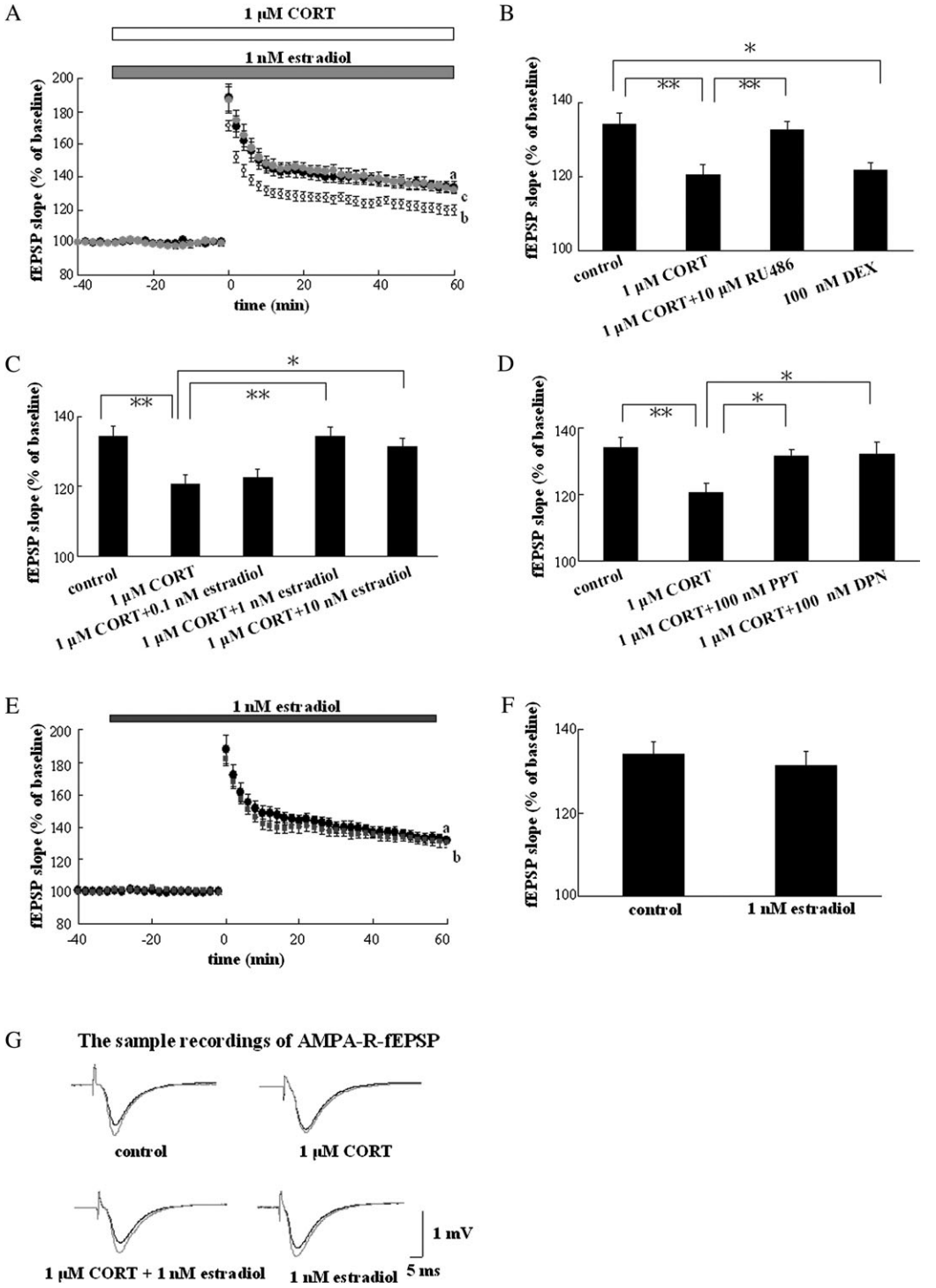

Figure 1. Rapid modulation of LTP by CORT and estradiol. (*A*) One micromolar CORT suppressed LTP and 1 nM estradiol rescued LTP from this CORT-induced suppression at CA3–CA1 synapses of acute slices. Vertical axis indicates the maximal fEPSP slope. Baseline is set at 100%. Open bar above the graph indicates the period of time during which CORT was administered. Gray closed bar above the graph indicates the period of time during which estradiol was administered. Curve a, control slices (black closed circle, $n = 10$); curve b, 1 μM CORT-treated slices (open circle, $n = 14$); and curve c, slices treated by 1 μM CORT plus 1 nM estradiol (Gray closed circle, $n = 6$). Illustrated data points and error bars represent the mean ± standard error mean from n independent slices. (*B*) Comparison of the modulation effect by CORT on LTP. From left to right: control slices (control, $n = 10$), 1 μM CORT-treated slices (1 μM CORT, $n = 14$), slices treated with 1 μM CORT and 10 μM RU486 (1 μM CORT + 10 μM RU486, $n = 6$), and 100 nM DEX-treated slices (100 nM DEX, $n = 5$). (*C*) Comparison of the modulation effect by estradiol on CORT-induced LTP suppression. From left to right: control slices (control, $n = 10$), 1 μM CORT-treated slices (1 μM CORT, $n = 14$), slices treated with 1 μM CORT and 0.1 nM estradiol (1 μM CORT + 0.1 nM estradiol, $n = 8$), 1 μM CORT and 1 nM estradiol (1 μM CORT + 1 nM estradiol, $n = 6$), and 1 μM CORT and 10 nM estradiol (1 μM CORT + 10 nM estradiol, $n = 10$). (*D*) Comparison of the modulation effect by ER agonists on CORT-induced LTP suppression. From left to right: control slices (control, $n = 10$), 1 μM CORT-treated slices (1 μM CORT, $n = 14$), slices treated with 1 μM CORT and 100 nM PPT (1 μM CORT + 100 nM PPT, $n = 10$), slices treated with 1 μM CORT and 100 nM DPN (1 μM CORT + 100 nM DPN, $n = 8$). (*E*) One nanomolar estradiol alone does not affect LTP at CA3–CA1 synapses of acute slices. Vertical axis indicates the maximal fEPSP slope. Baseline is set at 100%. Gray closed bar above the graph indicates the period of time during which estradiol was administered. Curve a, control slices (black closed circle, $n = 10$); curve b, 1 nM estradiol-treated slices (Gray closed square, $n = 11$). (*F*)

induction of LTP (Supplementary Fig. S2*B*), indicating that the CORT-induced suppression of LTP might not be dependent on presynaptic processes.

Estradiol Abolishes CORT-induced LTP Suppression

To examine the effect of estradiol on the CORT-induced LTP suppression, estradiol and CORT were coperfused. From 30 min before tetanic stimulation, 1 μM CORT and 0.1, 1, or 10 nM estradiol were coperfused. A dose-dependent rescue effect by estradiol was observed in LTP (Fig. 1*C*). The magnitude of LTP was 121 ± 3% for slices treated with 1 μM CORT (n = 14 slices), 122 ± 3% for slices treated with 0.1 nM estradiol plus 1 μM CORT (n = 8), 134 ± 3% for slices treated with 1 nM estradiol plus 1 μM CORT (n = 6), and 131 ± 2% for slices treated with 10 nM estradiol plus 1 μM CORT (n = 10). A significant rescue of LTP from the CORT-induced suppression by 1 or 10 nM estradiol was observed.

To assess whether estradiol rescues LTP from the CORT-induced suppression by modulating presynaptic activity, PPF was analyzed. Because there was no significant difference in PPF ratio, between before and after estradiol–CORT perfusion and after induction of LTP (Supplementary Fig. S2*C*), the effect of estradiol on CORT-induced suppression might not be dependent on presynaptic mechanisms.

Estrogen Receptor Agonists Abolish CORT-induced LTP Reduction

To identify the estrogen receptors, which drive the current effects, we coperfused CORT with the ERα-specific agonist PPT (Stauffer et al. 2000) or with the ERβ-specific agonist DPN (Meyers et al. 2001). Not only PPT but also DPN abolished CORT-induced LTP suppression. The magnitude of LTP was restored to 132 ± 2% (n = 10 slices) for slices treated with 100 nM PPT plus 1 μM CORT and to 132 ± 4% (n = 8) for slices treated with 100 nM DPN plus 1 μM CORT (Fig. 1*D*). When the dose of PPT or DPN was as low as 10 nM, they could not rescue LTP from CORT-induced suppression.

As far as 12-week-old adult male Wistar rats are concerned, estradiol alone (Fig. 1*E*,*F*) did not induce the rapid elevation of baseline fEPSP upon the perfusion of estradiol, and therefore, estradiol alone did not affect LTP. These results are in good agreement with previous results indicating that estradiol alone did not affect baseline fEPSP and/or LTP in 12-week-old adult male Wistar rat hippocampus (Ito et al. 1999; Mukai et al. 2007; Ogiue-Ikeda et al. 2008).

Suppression by CORT of NMDA-R-fEPSP

To investigate the effects of CORT at postsynapses, we measured CORT effects on the slope of the NMDA-R-fEPSP. The NMDA-R-fEPSP slope was selectively measured by the presence of the AMPAR inhibitor, CNQX at 10 μM. Upon perfusion of 1 μM CORT for slices, the NMDA-R-fEPSP slope decreased immediately, reaching 87 ± 2% of baseline (n = 6 slices) at 20 min after the onset of perfusion (Fig. 2*A*). This decrease was abolished by the washout of CORT.

When CORT was perfused with the GR antagonist RU486, no decrease was observed in the NMDA-R-fEPSP slope (102 ± 3% of baseline, n = 5), indicating that the suppression effect by CORT was induced via GR (Fig. 2*B*).

The downstream signaling of GR was examined by the application of a calcineurin inhibitor, cyclosporin A (CsA). The suppression effect of NMDA-R-fEPSP by CORT was abolished by coprefusion of 10 μM CsA with CORT (101 ± 4% of baseline, n = 8), indicating that the suppression effect by CORT was induced via calcineurin (Fig. 2*C*). PPF ratio was unchanged by perfusion of 1 μM CORT (Supplementary Fig. S2*E*).

Estradiol Abolishes CORT-induced Suppression of NMDA-R-fEPSP

To examine the rescue effect by estradiol on the NMDA-R-fEPSP slope from the CORT-induced decrease, 1 nM estradiol or an agonist of estrogen receptors was coperfused with 1 μM CORT. The relative magnitude of the NMDA-R-fEPSP slope was 87 ± 2% for slices treated with only 1 μM CORT (n = 6 slices) (Fig. 2*A*), 102 ± 2% for slices treated with 1 nM estradiol plus 1 μM CORT (n = 8) (Fig. 3*A*), 100 ± 2% for slices treated with 100 nM PPT plus 1 μM CORT (n = 5) (Fig. 3*B*), and 102 ± 4% for slices treated with 100 nM DPN plus 1 μM CORT (n = 5) (Fig. 3*C*) at 20 min after the onset of perfusion. Upon washing out of estradiol, PPT, or DPN, the CORT-induced decrease of NMDA-R-fEPSP slope again appeared (Fig. 3*A*,*B*,*C*). Note that estradiol alone had no effect on the NMDA-R-fEPSP slope (Fig. 3*D*). PPF ratio was unchanged by perfusion of 1 nM estradiol with 1 μM CORT (Supplementary Fig. S2*F*).

mitogen-activated protein Kinase Inhibitor Prevents Estradiol-induced Abolition of CORT-induced Suppression of NMDA-R-fEPSP

Coperfusion of 10 μM U0126, an inhibitor of mitogen-activated protein (MAP) kinase, with 1 nM estradiol plus 1 μM CORT completely inhibited the estradiol-induced abolition of the CORT-induced decrease of the NMDA-R-fEPSP slope (87 ± 2%, n = 6 slices) at 20 min after the onset of CORT and estradiol perfusion (Fig. 3*E*).

NR2B Inhibitor Prevents Estradiol-induced Abolition of CORT-induced Suppression of NMDA-R-fEPSP

To investigate the involvement of NR2B in the mechanism of the rescue effect by estradiol on the NMDA-R-fEPSP slope from the CORT-induced decrease, NR2B inhibitor Ro25-6981 at 1 μM was perfused from 1 h before the perfusion of CORT and estradiol. Under Ro25-6981 perfusion, the rescue effect by estradiol from CORT-induced decrease of the NMDA-R-fEPSP slope was abolished (89 ± 2%, n = 6 slices) at 20 min after the onset of CORT and estradiol perfusion (Fig. 3*F*).

Ultrastructural Analysis for Synaptic, Extranuclear and Nuclear Localization of GR

To explain the site of rapid modulation of LTP or NMDA-R-fEPSP slope at CA3–CA1 synapses by the activation of GR, a clarification of the subcellular localization (particularly the synaptic or extranuclear localization) of GR in CA1 pyramidal cells is essential. The synaptic, extranuclear, and nuclear

Comparison of the modulation effect by estradiol on LTP. From left to right: control slices (control, n = 10) and 1 nM estradiol-treated slices (1 nM estradiol, n = 11). (*G*) AMPA-R-fEPSP traces showing sample recordings taken prior to (t = −30 min, black) and after (t = 60 min, gray) tetanic stimulation. Control, 1 μM CORT, 1 μM CORT + 1 nM estradiol, and 1 nM estradiol correspond to fEPSP trace of control slice, 1 μM CORT-treated slice, slice treated with 1 μM CORT and 1 nM estradiol, and 1 nM estradiol-treated slice. In (*B*–*D*) and (*F*), vertical axis is the average of the fEPSP slope during the 10 min from t = 50 to t = 60 min. Statistical significance was confirmed via ANOVA followed by Tukey–Kramer's method (*P < 0.05; **P < 0.01) in (*B*–*D*), and via Student's t-test in (*F*). Note that steroids did not affect the baseline fEPSP slope before LTP induction.

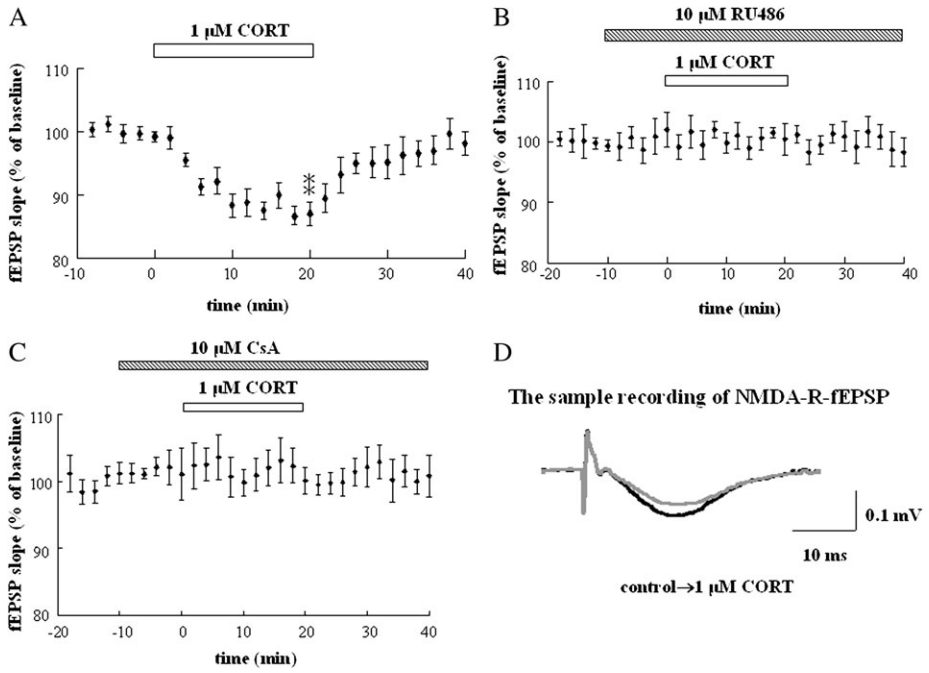

Figure 2. Rapid suppression by CORT of the NMDA-R-fEPSP slope. (*A*) Time dependence of NMDA-R-fEPSP slope upon perfusion of 1 μM CORT for 20 min. The suppression by CORT disappeared after washing out of CORT. Baseline (average over the 10 min prior to steroid perfusion) is set at 100%. (*B*) Abolition of the CORT effect on NMDA-R-fEPSP slope following the perfusion of 10 μM GR antagonist RU486 (perfused as indicated by the hatched bar). (*C*) Abolition of the CORT effect on NMDA-R-fEPSP slope following the perfusion of 10 μM CsA, a calcineurin inhibitor (perfused as indicated by the hatched bar). (*D*) NMDA-R-FEPSP traces showing sample recordings taken prior to ($t = 0$ min, black) and after ($t = 20$ min, Gray) perfusion of steroids. Control→1 μM CORT corresponds to the fEPSP trace of a 1 μM CORT-treated slice. Perfusion period of CORT is indicated by the open bar in (*A–C*). Statistical significance was confirmed via repeated measures ANOVA, followed by a paired *t*-test corrected by Bonferroni's method (*$P < 0.05$; **$P < 0.01$). The paired *t*-test was used for multiple comparisons between the baseline value (before steroid perfusion), $t = 20$ min value and $t = 40$ min value.

localization of GR was clarified via ultrastructural investigations using GR IgG (1/3000). An immunoelectron microscopic analysis using postembedded immunogold was performed to determine the localization of GR immunoreactivity in the hippocampal CA1 pyramidal cells of adult male rats. GR was localized not only in the nuclei but also in both the axon terminals and dendritic spines of pyramidal cells (Fig. 4*A*,*B*). Gold particles were clustered in the post- and presynaptic compartments as well as the nuclei, dendrites, and cytoplasm. At postsynapses, gold particles were distributed within the cytoplasm of the spine head. In some cases, gold particles were affiliated within the postsynaptic density (PSD). Significant labeling along dendrites was also observed (Fig. 4*C*). In contrast, many fewer gold particles were observed in axons. In glial-like cells, gold particles were not clearly recognized. To ensure specific labeling, multiple labeling (3 or more) of immunogold in the pre- and postsynaptic compartments was confirmed. For a search of immunogold-labeled GR proteins, we used at least 100 images. Each image contained several synapses among which at least one synapse expressed GR particles. We also observed some synapses in one image that did not express GR particles. Consequently, we observed roughly 25–30% of synapses that expressed GR particles. Preadsorption of the antibody with GR antigen (30 μg/mL) resulted in the disappearance of immunoreactivity.

Western Blot Analysis of GR in Synaptic and Extranuclear Fractions

Extended analysis indicated that GR was certainly localized in the purified PSD fraction, which was characterized by PSD-95, as described previously (Mukai et al. 2007). GR was observed in presynaptic membrane-rich fraction (PRE, characterized by synaptophysin), high-density membrane fraction (HDM, containing microsomes), PSD fraction, and cytoplasmic fraction (Cyt) (Fig. 4*D*). The total integrated amount of GR was largest in the Cyt fraction, relative to other fractions.

Mass-spectrometric Analysis of CORT and Estradiol in Slices

To examine the steroid concentrations in the hippocampal acute slices used for electrophysiological investigations, the concentration of CORT or estradiol was determined in these hippocampal slices after 2-h incubation with steroid-free ACSF by mass-spectrometric analysis. Chromatographic profiles for the fragmented ion of CORT with $m/z = 121$ (Supplementary Fig. S3*A*) showed a clear peak with a retention time of 5.75 min (Fig. 5*A*), which was the same retention time obtained for the fragmented ion of standard CORT (Fig. 5*B*). Chromatographic profiles for the fragmented ion of estradiol-PFBz-picolinoyl with $m/z = 339$ (Supplementary Fig. S3*B*) showed a clear peak with a retention time of 7.01 min (Fig. 5*C*), which was the same retention time obtained for the fragmented ion of the standard estradiol derivative (Fig. 5*D*). In hippocampal acute slices incubated for 2 h with steroid-free ACSF, the levels of estradiol and CORT were 0.13 ± 0.02 ($n = 5$) and 0.67 ± 0.07 ($n = 5$) ng/g wet weight (i.e., 0.48 ± 0.09 and 1.93 ± 0.20 nM), respectively. Because the estradiol level remained higher than 0.1 nM after the incubation in ACSF, exogenous application of 0.1 nM estradiol could not rescue LTP from CORT-induced suppression (Fig. 1*C*).

Discussion

The current study demonstrates that estradiol rapidly abolished the acute GR-mediated suppression of LTP as well as NMDA-R-

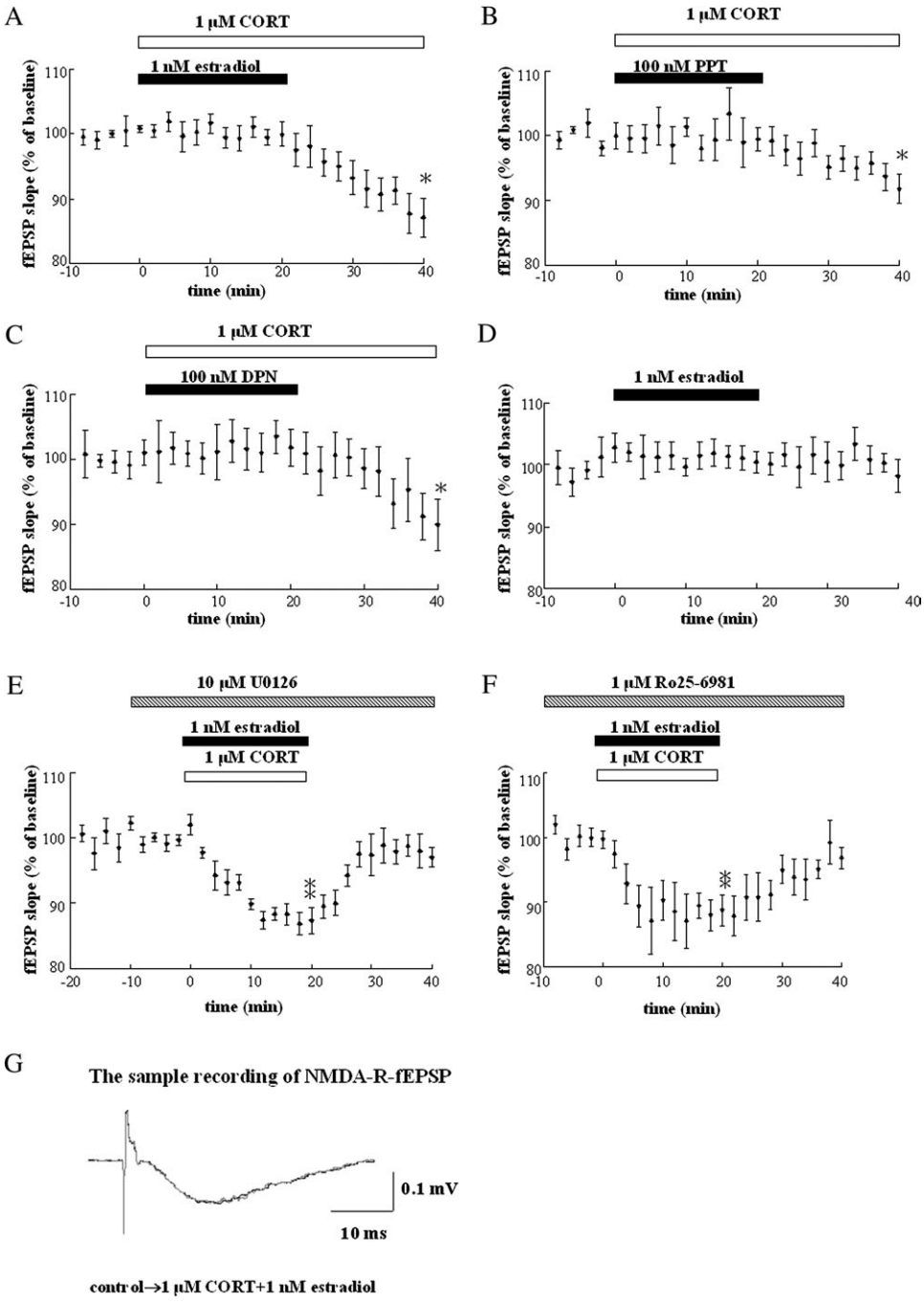

Figure 3. Estradiol rescued NMDA-R-fEPSP from CORT-induced suppression. (*A*) Abolition of the CORT-induced suppression of NMDA-R-fEPSP slope by 1 nM estradiol. (*B*) Abolition of the CORT effect on NMDA-R-fEPSP slope by 100 nM PPT. (*C*) Abolition of the CORT effect on NMDA-R-fEPSP slope by 100 nM DPN. (*D*) Estradiol alone has no effect on NMDA-R-fEPSP. (*E*) Abolition of the estradiol effect on CORT-induced suppression of NMDA-R-fEPSP slope following the perfusion of 10 μM U0126, an MAP kinase inhibitor (perfused as indicated by the hatched bar). (*F*) Abolition of the estradiol-induced rescue effect on CORT-induced suppression of NMDA-R-fEPSP slope following the perfusion of 1 μM Ro25-6981, an NR2B inhibitor (perfused as indicated by the hatched bar). Ro25-6981 was perfused from 1 h before the onset of CORT and estradiol perfusion. (*G*) NMDA-R-FEPSP traces showing sample recordings taken prior to ($t = 0$ min, black) and after ($t = 20$ min, gray) perfusion of steroids. Control → 1 μM CORT + 1 nM estradiol corresponds to the fEPSP trace of a slice treated with 1 μM CORT and 1 nM estradiol. In (*A*–*F*), the period of CORT perfusion is indicated by the open bar and that of estradiol or ER agonists perfusion by the closed bar. Note that estradiol, PPT, or DPN alone had no effect on the NMDA-R-fEPSP slope. Statistical significance was confirmed via repeated measures ANOVA, followed by a paired *t*-test corrected by Bonferroni's method (*$P < 0.05$; **$P < 0.01$). The paired *t*-test was used for multiple comparisons between the baseline value (before steroid perfusion), $t = 20$ min value and $t = 40$ min value.

fEPSP. This is a good simulation of what happens in memory processes upon acute stress in physiological conditions because estradiol is always present in the hippocampus independent of gender. Both MAP kinase and calcineurin were involved downstream of these events. We examined NMDA-R-fEPSP because it is considered to be essentially involved in the postsynaptic mechanisms of LTP induction process in CA3–CA1 synapses. The synaptic or extranuclear localization of GR and ERα, identified via immunoelectron microscopic analysis and western blot, supports the synaptic mechanisms of rapid effects by estradiol and CORT

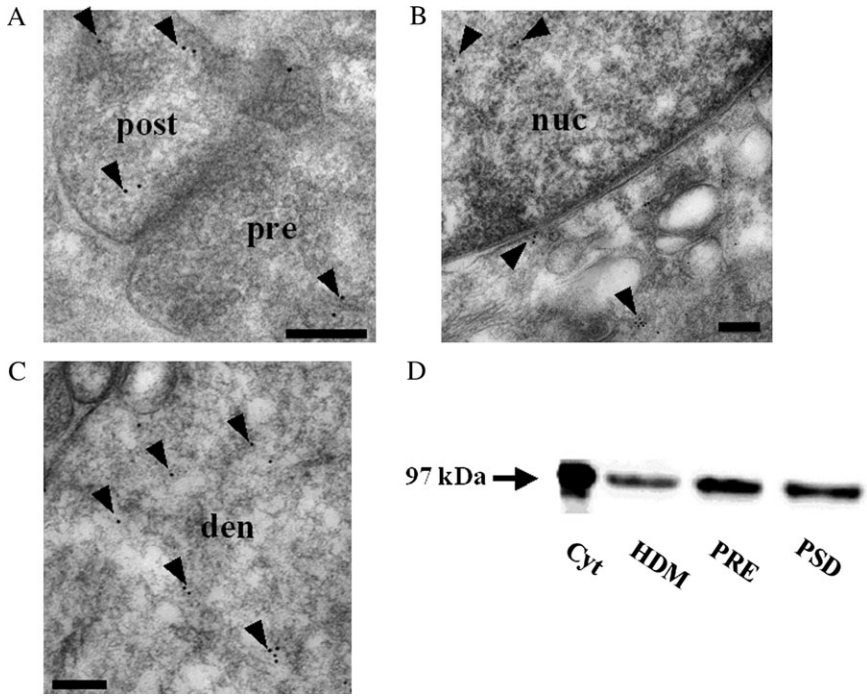

Figure 4. (*A–C*) Immunoelectron microscopic analysis of the distribution of GR within the axospinous synapses and dendrites in the stratum radiatum and nuclei of pyramidal cells in the CA1 region. A search for immunogold-labeled GR proteins was performed for at least 30 synapses at the CA1 region from more than 100 independent images. Gold particles (arrowheads), specifically indicating the presence of GR, were localized in the pre- and postsynaptic regions. In dendritic spines, gold particles were found within the spine head and, in some cases, were associated with PSD regions (*A*), axospinous synapses of pyramidal cells in the stratum radiatum in the CA1 region. Gold particles were also localized in the nuclei (*B*). In dendrites, gold particles were often found in the cytoplasmic space (*C*). A 1:3000 dilution of antiserum was used to prevent nonspecific labeling. Pre, presynaptic region; post, postsynaptic region; nuc, nucleus; den, dendrite. Scale bar, 200 nm. (*D*) Western blot analysis of GR in subcellular fractions of the hippocampus. From left to right: Cyt, HDM fraction, PRE, and PSD. The hippocampal cytosol was used as positive control for GR expression (Komatsuzaki et al. 2005). The amount of protein applied was 20 μg for each lane.

(Komatsuzaki et al. 2005; Warner and Gustafsson 2006). The exogenously applied 1 nM estradiol was effective in these rescue experiments because the estradiol concentration in slices (0.48 nM) used for electrophysiological measurements was much lower than 1 nM due to the release of endogenous estradiol to ACSF.

Postsynapse-dependent Effects by Estradiol and CORT

PPF analysis was performed in order to judge whether or not the drug might affect presynapses (Katz and Miledi 1968; Zucker 1989; Manabe et al. 1993; Isaacson and Walmsley 1995). For all of the steroids and agonists examined, the PPF ratio showed no change in LTP and NMDA-R-fEPSP measurements, suggesting that the CORT-induced LTP reduction and estradiol-induced restoration effects may be postsynapse dependent, though these results do not completely rule out a presynaptic dependency.

CORT Rapidly Suppresses LTP and NMDA-R-fEPSP via Postsynaptic/Extranuclear GR and Calcineurin

The involvement of GR in the CORT effect was proven by using a GR antagonist RU486 and a GR agonist DEX. RU486 blocked CORT-induced LTP suppression, while DEX induced LTP suppression (Fig. 1*B*). CORT-induced suppression of NMDA-R-fEPSP was blocked by RU486 as well as an inhibitor of calcineurin, CsA (Fig. 2*B,C*). Calcineurin is known to desensitize an NMDAR subunit NR2A via dephosphorylation of a serine residue (Krupp et al. 2002). Therefore, the signaling pathway may be CORT → GR → calcineurin → inactivation of NMDAR → reduction of Ca^{2+} influx during tetanic stimulation → reduced phosphorylation of AMPAR → LTP suppression (Fig. 6*A*). Using western immunoblot analysis, we observed GR in the PSD fraction (Fig. 4*D*). We also observed GR at synapses and extranuclei via immunoelectron microscopic analysis (Fig 4*A,C*). These results suggest that the rapid modulation of LTP by CORT is mediated by postsynaptic or extranuclear GR.

Estradiol Abolishes CORT-induced Suppression of LTP and NMDA-R-fEPSP via Synaptic/Extranuclear Estrogen Receptors and MAP Kinase

Slow neuroprotection by estradiol has been extensively investigated. Estradiol slowly protects the neural death induced by several neurotoxins as well as a high dose of a GR agonist DEX in the time scale of 24 h, depending on nuclear GR and ER pathways (Haynes et al. 2003). However, our observation of rapid estradiol effects (<1 h) on the abolishment of CORT-induced LTP reduction is too rapid for nuclear GR and ER pathways. It is indicated from NMDA-R-fEPSP experiments that the rapid LTP reduction by CORT is induced via decrease of Ca^{2+} influx during tetanic stimulation into postsynapses through NMDARs (Fig. 6*A*); therefore, the presence of estradiol may rescue synaptic transmission by restoration of the Ca^{2+} influx via NMDARs during tetanic stimulation. The pathway of the rapid effect of estradiol should involve ERα or ERβ at the synapses (or in extranuclei) because an ERα agonist PPT and an ERβ agonist DPN showed clear rescue effects on LTP and NMDA-R-fEPSP slope from the CORT-induced suppression. Recently, we found ERα localization at CA1 synapses and dendrites by immunoelectron microscopy, using purified ERα antibody RC-19 (Mukai et al. 2007).

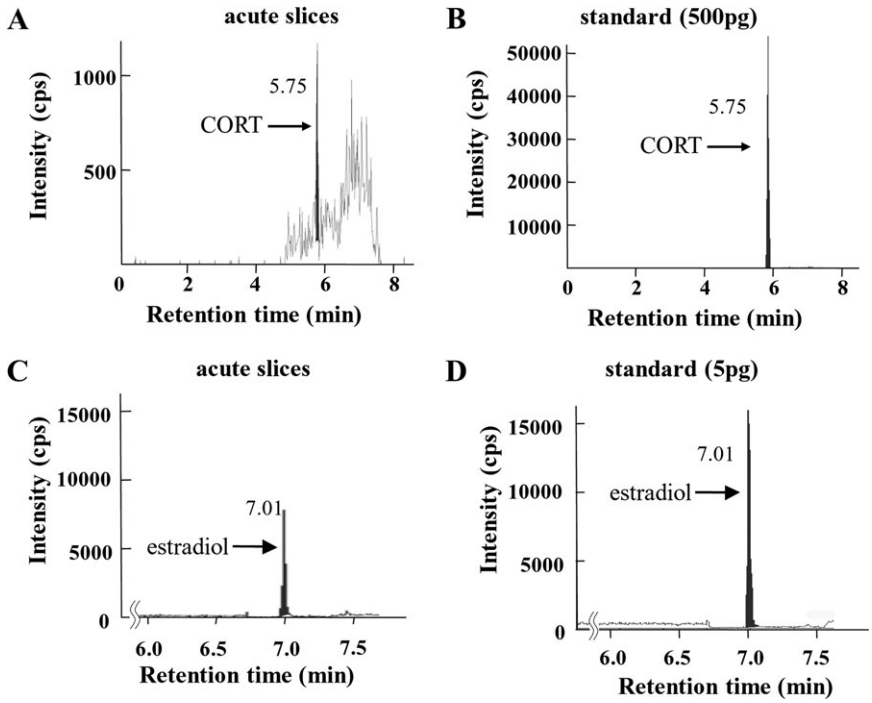

Figure 5. Mass-spectrometric analysis of CORT and estradiol in acute slices. LC-MS/MS ion chromatograms of CORT are shown in (*A–B*), those of estradiol are shown in (*C–D*). (*A*) Shaded portion indicates the fragmented ion of CORT ($m/z = 121$) extracted from acute slices of the hippocampus incubated for 2 h in steroid-free ACSF. (*B*) Shaded portion indicates the chromatograms of the fragmented ions of 500 pg of standard CORT. (*C*) Shaded portion indicates the fragmented ion of estradiol-PFBz-picolinoyl ($m/z = 339$) derivatized from estradiol extracted from acute slices of the hippocampus incubated for 2 h in steroid-free ACSF. (*D*) Shaded portion indicates the fragmented ion of estradiol-PFBz-picolinoyl derivatized from 5 pg of standard estradiol. Vertical axis indicates the detected intensity of the fragmented ions. Horizontal axis indicates the retention time of the fragmented ions, $t = 5.75$ min for CORT and $t = 7.01$ min for estradiol-PFBz-picolinoyl, respectively. The time at injection into the LC system was defined as $t = 0$ min. Average weight of the whole hippocampus used for each determination was approximately 0.14 g per animal.

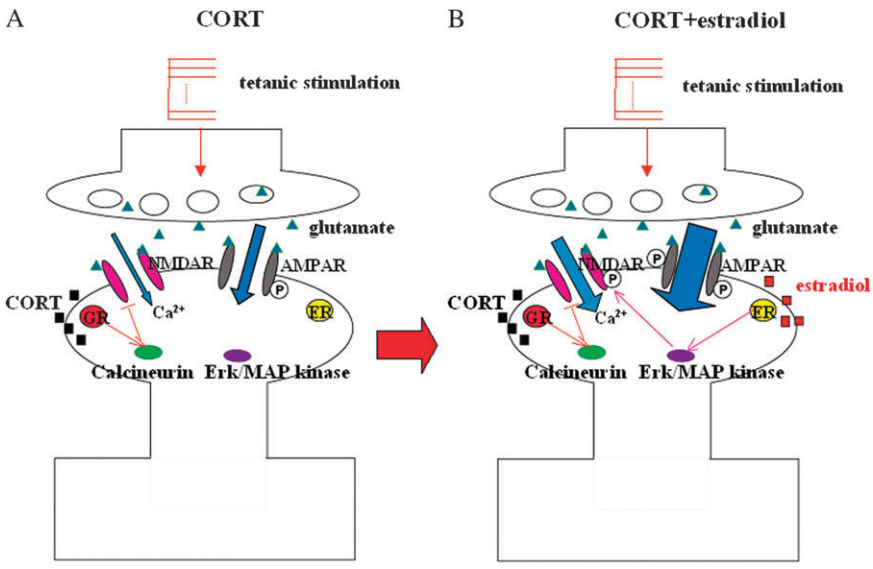

Figure 6. Hypothetical mechanisms of modulation of LTP by CORT and estradiol. (*A*) CORT-induced LTP suppression. An application of 1 μM CORT drives the following signaling pathway: CORT → GR → calcineurin → NR2A dephosphorylation. CORT finally dephosphorylates an NMDAR subunit NR2A. Upon tetanic stimulation, AMPAR is not sufficiently phosphorylated at the residue of serine 831 because CORT already suppressed NMDAR-derived Ca^{2+} current by dephosphorylation of NR2A, resulting in the suppression of LTP induction. (*B*) Rescue by estradiol of LTP from CORT-induced suppression. The application of 1 nM estradiol drives the following signaling pathway: estradiol → ERα or ERβ → MAP kinase → NR2B phosphorylation. Estradiol finally phosphorylates an NMDAR subunit NR2B. Upon tetanic stimulation, estradiol-induced restoration of NMDAR derived Ca^{2+} current by phosphorylation of NR2B causes sufficient phosphorylation of AMPAR at the residue of serine 831, resulting in the restoration of LTP induction.

The rapid action of estradiol is driven via MAP kinase because U0126 completely suppressed the estradiol-induced restoration effect on NMDA-R-fEPSP. Since MAP kinase is localized in the PSD fraction (Mukai et al. 2007), the activation of MAP kinase probably occurs within the postsynapses. Application of estradiol rapidly phosphorylates tyrosine 1472 of NR2B (an NMDAR subunit) (Dominguez et al. 2007). We also demonstrated that NR2B inhibitor Ro25-6981 significantly

suppressed the estradiol-induced restoration effect on NMDA-R-fEPSP. We therefore hypothesize that the signaling pathway is estradiol→ERα or ERβ→MAP kinase→activation of NMDAR by phosphorylation of NR2B→rescue of Ca^{2+} influx from CORT-induced suppression during tetanic stimulation →restoration of phosphorylation of AMPAR→LTP restoration (see Fig. 6*B*). Thus, estradiol restores AMPA receptor-derived field excitatory postsynaptic potential (AMPA-R-fEPSP) enhancement by tetanic stimulation due to restoration of phosphorylation of AMPARs. The contribution of NR2B modulation by estradiol to LTP induction is supported by earlier studies. Subcutaneous 2-time injections of estradiol to ovariectomized female rats with interval of 24 h genomically enhance NR2B-derived excitatory postsynaptic current at CA3–CA1 synapses after 24–48 h of the second injection (Smith and McMahon 2006; Snyder et al. 2011), resulting in the increase of LTP (Smith and McMahon 2006). Contrary to this genomic effect by estradiol, it is important that neither estradiol alone nor ER agonist alone (PPT or DPN) affected LTP or NMDA-R-fEPSP in the current study, implying that estradiol works particularly as a rescue signal from some suppression with the nongenomic mechanism. MAP kinase activation by estradiol is shown in mouse neonatal cortex (Toran-Allerand et al. 2002). Practically, we observed rapid estradiol-induced phosphorylation in hippocampal slices.

The current conclusion about estradiol-induced rescue effects on CORT-induced suppressions is supported by the control results that estradiol alone did not affect baseline fEPSP in the case of LTP experiments and NMDA-R-fEPSP experiments concerning 12-week-old (3-month-old) adult Wistar rats (Fig. 1*E*) (Ito et al. 1999; Ogiue-Ikeda et al. 2008). On the other hand, several studies have shown that estradiol alone rapidly increases baseline fEPSP (thereby enhances LTP) in the hippocampus of 4–6-week-old or 200–350 g (roughly 6–8-week-old) Sprague Dawley rats (Foy et al. 1999; Bi et al. 2000; Kramar et al. 2009). Therefore, these differences about estradiol-induced elevation of baseline fEPSP may depend on the age (12 weeks old or 4–8 weeks old) or strain (Wistar or Sprague Dawley) of rats. Concerning 4-week-old male Wistar rats, we sometimes (less than 20% possibility) observed the rapid baseline fEPSP elevation upon estradiol alone perfusion (Kawato 2004; Mukai et al. 2006; Ogiue-Ikeda et al. 2008). On the other hand, concerning 12-week-old male Wistar rats, Ito's group demonstrates no rapid baseline elevation upon estradiol alone perfusion as well as no enhancement of LTP (Ito et al. 1999). Interestingly, Foy and Thompson's group shows no rapid basal fEPSP elevation (<3% elevation) upon estradiol alone perfusion in case of 3–5-month-old as well as 18–24-month-old Sprague Dawley rats (Vouimba et al. 2000). Therefore, estradiol alone may have the significant effect of rapid baseline elevation of synaptic transmission on younger rats (4–8 weeks old) and may not have the effect on older adult rats (12 weeks old or elder).

Steroid Levels in Slices Vary by the Incubation or Perfusion with ACSF

The basal steroid levels in slices used for electrophysiological measurements must be known. We observed that the concentrations of estradiol and CORT in acute slices were 0.48 and 1.9 nM, respectively. Since the endogenous level of estradiol in the intact hippocampus is roughly 8 nM (Hojo et al. 2009), the estradiol level might be reduced due to release into ACSF during 2-h incubation. Therefore, in such estradiol-depleted slices, a 1-nM estradiol application can induce significant restoration effects on LTP and NMDA-R-fEPSP. Due to an endogenous high level of estradiol in cultured neurons, only a high concentration of applied estradiol at 100 nM shows proliferative effects on hippocampal-cultured granule cells, but no effect is observed when applied estradiol is 0.1 nM (Fester et al. 2006).

Estradiol is efficiently released from the slices by incubation or perfusion of steroid-free ACSF. The spine density of CA1 pyramidal cells is increased by a 1-nM estradiol application for 2 h and returns to the control level following washing out of estradiol (Mukai et al. 2007). The current study also demonstrated the reversibility of the rapid effect of estradiol. The rescue by 1 nM estradiol of NMDA-R-fEPSP from the suppression by 1 μM CORT was diminished following the washing out of estradiol.

Concerning CORT level, the CORT concentration in the freshly isolated whole hippocampus was very high at roughly 430 nM (see Supplementary Results and Discussion). This high CORT level is probably induced by the penetration of elevated plasma CORT (1–2 μM), due to ether stress for 1 min before sacrifice (Tohei et al. 1997), into the hippocampus. Note that 1–2 μM CORT is above the upper limit capacity (roughly 400–600 nM) of CORT-binding globulin (Breuner and Orchinik 2002).

The current study suggests that such a high concentration of CORT (430 nM) can be decreased to a very low level of 1.9 nM in acute slices by incubation in ACSF due to the release of CORT to ACSF. The following results can be interpreted by such an easy release of CORT. One to 10 μM CORT rapidly suppresses the amplitude of the population spike of CA1 pyramidal cells, and this suppression disappears following washing out of CORT (Vidal et al. 1986). The suppression of NMDA-R-fEPSP by 1 μM CORT was diminished by washing out of CORT by perfusion (Fig. 2*A*).

From the current study, it is deduced that moderate acute stress may be rescued by endogenous estradiol in the hippocampus in vivo (roughly 8 nM). An earlier study indicates that acute CORT secretion induced by water maze training impairs the performance of water maze test in female rats but not in male rats (Beiko et al. 2004). Endogenous level of estradiol in the hippocampus is much higher in male rats (roughly 8 nM) than in female rats (roughly 0.5–1.7 nM, which varies in accordance with estrus cycle) (Hojo et al. 2009). Taken together, it is suggested that sufficiently high level of endogenous estradiol in the male hippocampus can rescue acute stress-induced memory impairment.

Supplementary Material

Supplementary material can be found at: http://www.cercor.oxfordjournals.org/

Notes

We thank Prof. Mitsuhiro Kawata (Kyoto Prefectural University of Medicine) for GR antibody. S. Homma and M. Okuyama (Aska Pharma Medical) are acknowledged for mass-spectrometric analysis. We also thank Prof. J. A. Rose (Ritsumeikan University) for critical reading of the manuscript. *Conflict of Interest*: None declared.

References

Adams MM, Fink SE, Shah RA, Janssen WG, Hayashi S, Milner TA, McEwen BS, Morrison JH. 2002. Estrogen and aging affect the subcellular distribution of estrogen receptor-alpha in the hippocampus of female rats. J Neurosci. 22:3608–3614.

Alfarez DN, Wiegert O, Joels M, Krugers HJ. 2002. Corticosterone and stress reduce synaptic potentiation in mouse hippocampal slices with mild stimulation. Neuroscience. 115:1119–1126.
Behl C, Widmann M, Trapp T, Holsboer F. 1995. 17-beta estradiol protects neurons from oxidative stress-induced cell death in vitro. Biochem Biophys Res Commun. 216:473–482.
Beiko J, Lander R, Hampson E, Boon F, Cain DP. 2004. Contribution of sex differences in the acute stress response to sex differences in water maze performance in the rat. Behav Brain Res. 151: 239–253.
Bi R, Broutman G, Foy MR, Thompson RF, Baudry M. 2000. The tyrosine kinase and mitogen-activated protein kinase pathways mediate multiple effects of estrogen in hippocampus. Proc Natl Acad Sci U S A. 97:3602–3607.
Breuner CW, Orchinik M. 2002. Plasma binding proteins as mediators of corticosteroid action in vertebrates. J Endocrinol. 175:99–112.
Chen Y, Dube CM, Rice CJ, Baram TZ. 2008. Rapid loss of dendritic spines after stress involves derangement of spine dynamics by corticotropin-releasing hormone. J Neurosci. 28:2903–2911.
Dominguez R, Liu R, Baudry M. 2007. 17-Beta-estradiol-mediated activation of extracellular-signal regulated kinase, phosphatidylinositol 3-kinase/protein kinase B-Akt and N-methyl-D-aspartate receptor phosphorylation in cortical synaptoneurosomes. J Neurochem. 101: 232–240.
Fester L, Ribeiro-Gouveia V, Prange-Kiel J, von Schassen C, Bottner M, Jarry H, Rune GM. 2006. Proliferation and apoptosis of hippocampal granule cells require local oestrogen synthesis. J Neurochem. 97: 1136–1144.
Foy MR, Xu J, Xie X, Brinton RD, Thompson RF, Berger TW. 1999. 17beta-estradiol enhances NMDA receptor-mediated EPSPs and long-term potentiation. J Neurophysiol. 81:925–929.
Gerges NZ, Aleisa AM, Schwarz LA, Alkadhi KA. 2004. Reduced basal CaMKII levels in hippocampal CA1 region: possible cause of stress-induced impairment of LTP in chronically stressed rats. Hippocampus. 14:402–410.
Gu Q, Moss RL. 1996. 17 beta-Estradiol potentiates kainate-induced currents via activation of the cAMP cascade. J Neurosci. 16: 3620–3629.
Haynes LE, Lendon CL, Barber DJ, Mitchell IJ. 2003. 17 Beta-oestradiol attenuates dexamethasone-induced lethal and sublethal neuronal damage in the striatum and hippocampus. Neuroscience. 120: 799–806.
Hirata R, Togashi H, Matsumoto M, Yamaguchi T, Izumi T, Yoshioka M. 2008. Characterization of stress-induced suppression of long-term potentiation in the hippocampal CA1 field of freely moving rats. Brain Res. 1226:27–32.
Hojo Y, Hattori TA, Enami T, Furukawa A, Suzuki K, Ishii HT, Mukai H, Morrison JH, Janssen WG, Kominami S, et al. 2004. Adult male rat hippocampus synthesizes estradiol from pregnenolone by cytochromes P45017alpha and P450 aromatase localized in neurons. Proc Natl Acad Sci U S A. 101:865–870.
Hojo Y, Higo S, Ishii H, Ooishi Y, Mukai H, Murakami G, Kominami T, Kimoto T, Honma S, Poirier D, et al. 2009. Comparison between hippocampus-synthesized and circulation-derived sex steroids in the hippocampus. Endocrinology. 150:5106–5112.
Isaacson JS, Walmsley B. 1995. Counting quanta: direct measurements of transmitter release at a central synapse. Neuron. 15:875–884.
Ito K, Skinkle KL, Hicks TP. 1999. Age-dependent, steroid-specific effects of oestrogen on long-term potentiation in rat hippocampal slices. J Physiol. 515(Pt 1):209–220.
Katz B, Miledi R. 1968. The role of calcium in neuromuscular facilitation. J Physiol. 195:481–492.
Kawato S. 2004. Endocrine disrupters as disrupters of brain function: a neurosteroid viewpoint. Environ Sci. 11:1–14.
Kawato S, Hojo Y, Kimoto T. 2002. Histological and metabolism analysis of P450 expression in the brain. Methods Enzymol. 357:241–249.
Komatsuzaki Y, Murakami G, Tsurugizawa T, Mukai H, Tanabe N, Mitsuhashi K, Kawata M, Kimoto T, Ooishi Y, Kawato S. 2005. Rapid spinogenesis of pyramidal neurons induced by activation of glucocorticoid receptors in adult male rat hippocampus. Biochem Biophys Res Commun. 335:1002–1007.
Kramar EA, Chen LY, Brandon NJ, Rex CS, Liu F, Gall CM, Lynch G. 2009. Cytoskeletal changes underlie estrogen's acute effects on synaptic transmission and plasticity. J Neurosci. 29:12982–12993.
Krupp JJ, Vissel B, Thomas CG, Heinemann SF, Westbrook GL. 2002. Calcineurin acts via the C-terminus of NR2A to modulate desensitization of NMDA receptors. Neuropharmacology. 42: 593–602.
Manabe T, Wyllie DJ, Perkel DJ, Nicoll RA. 1993. Modulation of synaptic transmission and long-term potentiation: effects on paired pulse facilitation and EPSC variance in the CA1 region of the hippocampus. J Neurophysiol. 70:1451–1459.
Meyers MJ, Sun J, Carlson KE, Marriner GA, Katzenellenbogen BS, Katzenellenbogen JA. 2001. Estrogen receptor-beta potency-selective ligands: structure-activity relationship studies of diarylpropionitriles and their acetylene and polar analogues. J Med Chem. 44: 4230–4251.
Mukai H, Takata N, Ishii HT, Tanabe N, Hojo Y, Furukawa A, Kimoto T, Kawato S. 2006. Hippocampal synthesis of estrogens and androgens which are paracrine modulators of synaptic plasticity: synaptocrinology. Neuroscience. 138:757–764.
Mukai H, Tsurugizawa T, Murakami G, Kominami S, Ishii H, Ogiue-Ikeda M, Takata N, Tanabe N, Furukawa A, Hojo Y, et al. 2007. Rapid modulation of long-term depression and spinogenesis via synaptic estrogen receptors in hippocampal principal neurons. J Neurochem. 100:950–967.
Murphy DD, Segal M. 1996. Regulation of dendritic spine density in cultured rat hippocampal neurons by steroid hormones. J Neurosci. 16:4059–4068.
Ogiue-Ikeda M, Tanabe N, Mukai H, Hojo Y, Murakami G, Tsurugizawa T, Takata N, Kimoto T, Kawato S. 2008. Rapid modulation of synaptic plasticity by estrogens as well as endocrine disrupters in hippocampal neurons. Brain Res Rev. 57: 363–375.
Pavlides C, Nivon LG, McEwen BS. 2002. Effects of chronic stress on hippocampal long-term potentiation. Hippocampus. 12: 245–257.
Reagan LP, McEwen BS. 1997. Controversies surrounding glucocorticoid-mediated cell death in the hippocampus. J Chem Neuroanat. 13:149–167.
Shibuya K, Takata N, Hojo Y, Furukawa A, Yasumatsu N, Kimoto T, Enami T, Suzuki K, Tanabe N, Ishii H, et al. 2003. Hippocampal cytochrome P450s synthesize brain neurosteroids which are paracrine neuromodulators of synaptic signal transduction. Biochim Biophys Acta. 1619:301–316.
Smith CC, McMahon LL. 2006. Estradiol-induced increase in the magnitude of long-term potentiation is prevented by blocking NR2B-containing receptors. J Neurosci. 26:8517–8522.
Snyder MA, Cooke BM, Woolley CS. 2011. Estradiol potentiation of NR2B-dependent EPSCs is not due to changes in NR2B protein expression or phosphorylation. Hippocampus. 21:398–408.
Stauffer SR, Coletta CJ, Tedesco R, Nishiguchi G, Carlson K, Sun J, Katzenellenbogen BS, Katzenellenbogen JA. 2000. Pyrazole ligands: structure-affinity/activity relationships and estrogen receptor-alpha-selective agonists. J Med Chem. 43:4934–4947.
Tohei A, Tomabechi T, Mamada M, Akai M, Watanabe G, Taya K. 1997. Effects of repeated ether stress on the hypothalamic-pituitary-testes axis in adult rats with special reference to inhibin secretion. J Vet Med Sci. 59:329–334.
Toran-Allerand CD, Guan X, MacLusky NJ, Horvath TL, Diano S, Singh M, Connolly ES, Jr., Nethrapalli IS, Tinnikov AA. 2002. ER-X: a novel, plasma membrane-associated, putative estrogen receptor that is regulated during development and after ischemic brain injury. J Neurosci. 22:8391–8401.
Vidal C, Jordan W, Zieglgansberger W. 1986. Corticosterone reduces the excitability of hippocampal pyramidal cells in vitro. Brain Res. 383:54–59.
Vouimba RM, Foy MR, Foy JG, Thompson RF. 2000. 17beta-estradiol suppresses expression of long-term depression in aged rats. Brain Res Bull. 53:783–787.
Warner M, Gustafsson JA. 2006. Nongenomic effects of estrogen: why all the uncertainty? Steroids. 71:91–95.

Watanabe Y, Gould E, McEwen BS. 1992. Stress induces atrophy of apical dendrites of hippocampal CA3 pyramidal neurons. Brain Res. 588:341–345.
Woolley CS, Gould E, McEwen BS. 1990. Exposure to excess glucocorticoids alters dendritic morphology of adult hippocampal pyramidal neurons. Brain Res. 531:225–231.
Zhang L, Rubinow DR, Xaing G, Li BS, Chang YH, Maric D, Barker JL, Ma W. 2001. Estrogen protects against beta-amyloid-induced neurotoxicity in rat hippocampal neurons by activation of Akt. Neuroreport. 12:1919–1923.
Zucker RS. 1989. Short-term synaptic plasticity. Annu Rev Neurosci. 12: 13–31.